JOURNAL OF MOLECULAR SPECTROSCOPY 156, 327–340 (1992)

Fourier Transform Jet-Emission Spectroscopy of the $A^2\Pi_i$–$X^2\Sigma^+$ Transition of CN

C. V. V. PRASAD AND P. F. BERNATH[1,2]

Centre for Molecular Beams and Laser Chemistry, Department of Chemistry, University of Waterloo, Waterloo, Ontario, Canada N2L 3G1

The red ($A^2\Pi_i$–$X^2\Sigma^+$) system of the CN free radical was produced in a jet-cooled corona-excited supersonic expansion of helium using diazoacetonitrile as a precursor molecule. This spectrum was recorded with the McMath Fourier transform spectrometer of the National Solar Observatory. A total of 27 bands with $v' = 8$ to 21 and $v'' = 1$ to 11 (LeBlanc bands) in the range 16 570–22 760 cm^{-1} were observed and rotationally analyzed. The line positions of this system were fitted along with those of the violet ($B^2\Sigma^+$–$X^2\Sigma^+$) system, infrared vibration–rotation data, and microwave data in a global fit. RKR potential energy curves were constructed for the $X^2\Sigma^+$, $A^2\Pi_i$, and $B^2\Sigma^+$ states of this molecule, and Franck–Condon factors were calculated for the vibrational bands of the A–X, B–A, and B–X systems.

INTRODUCTION

For more than a century the CN radical has been produced in the laboratory from a wide range of sources and has also been found to occur in many different celestial objects. In the laboratory CN molecules are produced in carbon arcs, active nitrogen after glows, flames, shock tubes, and electrical discharges. Recently, with the development of cold sources using the corona-excited supersonic jet expansion technique, there has been a renewed interest in the electronic spectrum of CN (*1–3*). The CN molecules produced by this technique are rotationally cold (30–50 K) but vibrationally hot (2000–6000 K). The molecules are excited to very high vibrational levels, but for each vibrational band only a few rotational lines with low rotational quantum numbers are observed. These low-J lines are often too weak and blended to be observed in traditional high-temperature sources. These few rotational lines are, in general, very sharp and well resolved, as well as free from local perturbations. Accurate T_v and B_v values for a large number of vibrational levels can be estimated, and this in turn is useful for the construction of RKR potential energy curves and the calculation of Franck–Condon factors.

CN molecules are found in many extraterrestrial sources such as the Sun (*4*), stellar atmospheres (*5, 6*), comets (*7*), dark interstellar clouds (*8, 9*), and diffuse interstellar clouds (*10–15*) by the techniques of microwave, infrared, and ultraviolet spectroscopy. The red ($A^2\Pi_i$–$X^2\Sigma^+$) system of CN is observed in emission from comets, and in absorption in late-type stars, carbon stars, and the Sun. The red system of CN is similar in occurrence and appearance to the Meinel band system of N_2^+ and the comet-tail system of CO^+, which are also due to $^2\Pi_i$–$^2\Sigma^+$ transitions.

Our interest in cold CN began with the observation of strong emission from the violet ($B^2\Sigma^+$–$X^2\Sigma^+$) system in the supersonic jet spectra of the CH_3N (*16, 17*) and

[1] Also: Department of Chemistry, University of Arizona, Tucson, AZ 85721.

[2] Camille and Henry Dreyfus Teacher-Scholar.

0022-2852/92 $5.00

CCN (*18*) free radicals. A corona excited supersonic jet expansion (*19*) of methyl azide and diazoacetonitrile precursors in He provided rotationally cold (30 K) emission spectra.

The red system of CN has been known for more than a century. However, Heurlinger (*20*) in 1920 was the first one to assign vibrational quantum numbers to the bands and Mulliken (*21*) in 1924 confirmed that these bands were due to CN. Asundi and Ryde (*22*) extended the observations of this system to 9400 Å and revised the vibrational numbering of Heurlinger (*20*) by increasing the upper state vibrational quantum numbers by two units. However, Herzberg and Phillips (*23*) observed the bands of this system in the near infrared out to 16 000 Å and increased the upper state vibrational quantum numbers by one more unit. This revised vibrational numbering is currently in use. At present the bands of this system are known with vibrational quantum numbers up to $v' = 25$ and $v'' = 14$ mainly due to the work of Douglas and Routly (*24*) and LeBlanc (*25*). Jenkins *et al.* (*26*) investigated the rotational structure of the red system and published the first set of rotational constants for the $A^2\Pi_i$ state. Douglas and Routly (*24*) and Davis and Phillips (*27*) also made extensive investigations of this system. For a detailed review of the enormous literature on the CN molecule, the reader is referred to the articles by Douglas and Routly (*24*) and Brocklehurst *et al.* (*28, 29*), as well as Huber and Herzberg's (*30*) book.

More recent rotational analyses of this system include the work of Cerny *et al.* (*31*) in which they investigated this system in the range 4000–11 000 cm^{-1} with a high-resolution Fourier transform spectrometer. Kotlar *et al.* (*32*) provided a deperturbed set of constants for the $v = 0$ to 12 vibrational levels of the $A^2\Pi_i$ state and $v = 0$ to 8 of the $X^2\Sigma^+$. Ito, Kuchitsu, and co-workers (*33–37*) have also investigated the perturbations of the $B^2\Sigma^+$ and $A^2\Pi_i$ states in detail. Very recently, Davis *et al.* (*38*) analyzed the vibration–rotation spectrum by Fourier transform spectroscopy, and Ito *et al.* (*39*) have analyzed the millimeter-wave spectrum of the vibrational levels $v =$ 3 to 10 of the $X^2\Sigma^+$ state. Prasad *et al.* (*1*) and Rehfuss *et al.* (*2*) investigated the violet (B–X) system. The latter also reported the observation of 54 bands of the A–X system throughout the red and infrared regions (2500–16 000 cm^{-1}), but no analysis has been published yet.

In the present study we investigated the red ($A^2\Pi_i$–$X^2\Sigma^+$) system of cold CN produced in a supersonic jet source in the spectral range 16 570–22 760 cm^{-1}. A total of 27 bands with $v' = 8$ to 21 and $v'' = 1$ to 11 were observed and their rotational structures were analyzed. Because of the very low rotational temperature of the molecules, only the T_v and B_v values could be estimated. The wavenumber data obtained for the red system was combined with the very recent experimental millimeter, infrared, and ultraviolet data in a simultaneous least-squares fit. The RKR potential energy curves for the X, A, and B states were derived, and Franck–Condon factors for the various vibrational bands of the red (A–X), LeBlanc (B–A), and violet (B–X) systems were calculated.

EXPERIMENTAL DETAILS

The red ($A^2\Pi_i$–$X^2\Sigma^+$) system of the CN molecule was produced in a corona-excited supersonic expansion of the Engelking (*19*) type. A potential of 3.5 kV was provided by a high voltage power supply through a ballast resistor of 2 MΩ to a 250-μm diameter tungsten wire. The tungsten wire ends 400 μm from a 250-μm-diameter pinhole nozzle in a quartz tube. Diazoacetonitrile was used as the precursor molecule (*18*) for the production of CN molecules and helium at a pressure of 4 atm was used

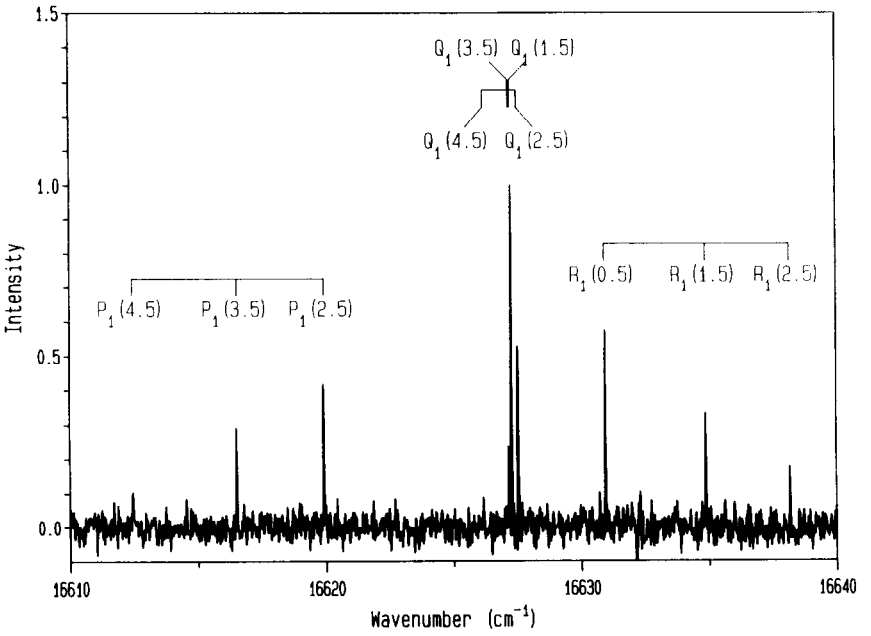

FIG. 1. The 8-3 band of the $A^2\Pi_{3/2}$–$X^2\Sigma^+$ transition of CN.

as the carrier gas. The pressure in the vacuum chamber was several hundred mTorr. The potential drop through the nozzle provided the electrical excitation to form a plasma. The subsequent expansion collisionally cooled the rotational motion of the molecules.

The radiation emitted by the rotationally cooled molecules was recorded by focusing the emission perpendicular to the molecular jet onto the entrance aperture of the McMath Fourier transform spectrometer of the National Solar Observatory at Kitt Peak. A total of four scans were co-added in 18 min of integration at a resolution of 0.025 cm^{-1}. Cooled GaAs photomultiplier tube detectors were used along with a 4300-Å red-pass filter and a 6000-Å blue-pass filter. This selection of filters and detectors allowed the spectrum to be recorded in the 16 000–23 000 cm^{-1} range.

In this spectrum bands of the Swan ($d^3\Pi_g$–$a^3\Pi_u$) system of C_2 and also those of the $\tilde{A}^2\Delta$–$\tilde{X}^2\Pi$ system of CCN were observed. For absolute wavenumber calibration the data from Doppler-limited dye laser studies of Kakimoto and Kasuya (*40*) on CCN were compared with those observed in our spectrum. As a double check, the spectral lines due to C_2 were compared with those of Suzuki *et al.* (*41*) and Curtis and Sarre (*42*) and the spectral line positions were found to be in good agreement.

ANALYSIS AND RESULTS

For the red ($A^2\Pi_i$–$X^2\Sigma^+$) system of the CN molecule the upper, $A^2\Pi_i$, state belongs to Hund's case (a) and the lower, $X^2\Sigma^+$, state to case (b). Twelve branches are expected, six each in the $A^2\Pi_{1/2}$–$X^2\Sigma^+$ and $A^2\Pi_{3/2}$–$X^2\Sigma^+$ subbands.

In the present study, because the CN molecules were rotationally very cold, only the transitions in the $A^2\Pi_{3/2}$–$X^2\Sigma^+$ subband were observed. In view of the very low rotational temperature of the CN molecules, only the first few rotational energy levels

TABLE I

Vacuum Wavenumbers (in cm^{-1}) for the Rotational Lines of the Bands of the Red ($A^2\Pi_i$–$X^2\Sigma^+$) System of the CN Molecule

J	$R_{11}(J)$	$Q_{11}(J)$	$P_{11}(J)$
		8-1 Band	
0.5	20636.854(-12)		
1.5	20640.763(32)	20633.116(2)	
2.5	20643.913(15)	20633.240(7)	20625.641(24)
3.5		20632.641(-12)	
		8-2 Band	
0.5	18620.736(-4)		
1.5	18624.636(-4)	18617.027(3)	
2.5	18627.869(-7)	18617.213(2)	18609.606(10)
3.5		18616.741(5)	18606.086(15)
4.5		18615.605(2)	18601.902(17)
5.5		18613.800(-12)	
6.5		18611.373(1)	
		8-3 Band	
0.5	16630.943(-4)		
1.5	16634.874(-9)	16627.267(1)	
2.5	16638.174(-16)	16627.525(0)	16619.919(10)
3.5		16627.155(0)	16616.502(12)
4.5		16626.159(-2)	16612.451(7)
5.5			16607.798(24)
		9-3 Band	
0.5	18213.622(-6)		
1.5	18217.471(-8)	18209.947(0)	
2.5	18220.659(-10)	18210.124(3)	18202.597(9)
3.5	18223.189(-12)	18209.633(-2)	18199.097(11)
4.5		18208.492(1)	18194.934(10)
5.5		18206.673(-19)	18190.111(8)
6.5			18184.639(8)
		10-3 Band	
0.5	19770.532(-6)		
1.5	19774.295(-8)	19766.880(22)	
2.5		19766.947(2)	19759.511(11)
3.5			19755.924(14)
4.5		19765.026(-9)	19751.640(15)
5.5		19763.057(12)	
		10-4 Band	
0.5	17807.115(-5)		
1.5	17810.903(-17)	17803.476(1)	
2.5	17814.043(-15)	17803.635(2)	17796.187(0)
3.5	17816.549(10)	17803.071(-58)	17792.714(11)
4.5		17801.953(-16)	
		11-4 Band	
0.5	19338.190(-4)		
1.5	19341.912(1)	19334.557(8)	
2.5	19344.941(8)	19334.627(3)	19327.280(18)
3.5		19334.018(15)	19323.718(24)
4.5		19332.695(3)	19319.448(14)
5.5			19314.487(6)

TABLE I—*Continued*

J	$R_{11}(J)$	$Q_{11}(J)$	$P_{11}(J)$
		11-5 Band	
0.5	17401.185(-15)		
1.5	17404.937(-15)	17397.584(-6)	
2.5	17408.023(-22)	17397.727(-7)	17390.372(-2)
3.5	17410.470(-10)	17397.213(-8)	17386.924(12)
4.5		17396.043(-9)	17382.801(9)
5.5		17394.191(-38)	
		12-4 Band	
0.5	20843.378(7)		
1.5	20847.019(18)	20839.741(15)	
2.5	20849.895(-6)	20839.741(27)	20832.458(20)
3.5		20838.993(20)	20828.825(41)
4.5		20837.531(25)	20824.410(7)
		12-5 Band	
0.5	18906.373(-3)		
1.5	18910.051(9)	18902.772(6)	
2.5	18913.013(0)	18902.826(1)	18895.569(20)
3.5		18902.186(-4)	18892.016(14)
4.5		18900.863(-2)	18887.765(4)
5.5		18898.854(1)	
		12-6 Band	
0.5	16995.827(-12)		
1.5	16999.526(-14)	16992.254(-10)	
2.5	17002.567(-16)	16992.386(-8)	16985.117(-2)
3.5		16991.861(-5)	16981.679(1)
4.5		16990.670(-12)	16977.585(6)
5.5			16972.816(-10)
		13-5 Band	
0.5	20385.576(10)		
1.5	20389.147(2)	20381.969(13)	
2.5	20392.047(42)	20381.969(37)	20374.772(34)
3.5		20381.193(11)	20371.140(31)
4.5		20379.698(-10)	20366.785(32)
5.5		20377.520(6)	20361.703(29)
		13-6 Band	
0.5	18475.033(5)		
1.5		18471.462(8)	
2.5		18471.506(5)	18464.324(16)
3.5		18470.857(-1)	18460.802(18)
4.5			18456.590(20)
		13-7 Band	
0.5	16590.985(-7)		
1.5	16594.639(-7)	16587.444(-9)	
2.5	16597.624(-21)	16587.570(-1)	16580.382(4)
3.5		16587.022(-13)	16576.965(4)
4.5		16585.850(4)	16572.878(-12)
		14-5 Band	
0.5	21838.716(13)		
1.5	21842.194(5)	21835.098(5)	
2.5		21834.992(19)	21827.889(13)
3.5			21824.177(27)

TABLE I—*Continued*

J	$R_{11}(J)$	$Q_{11}(J)$	$P_{11}(J)$
		14-7 Band	
0.5	18044.106(-23)		
1.5	18047.668(-19)	18040.583(-8)	
2.5	18050.533(-18)	18040.583(-30)	18033.506(-10)
3.5		18039.935(-5)	18030.001(-2)
4.5		18038.580(3)	18025.793(-3)
5.5		18036.503(-22)	
		15-7 Band	
0.5	19471.026(-1)		
1.5	19474.493(-8)	19467.490(1)	
2.5	19477.240(-8)	19467.422(-5)	19460.417(4)
3.5		19466.637(0)	19456.834(17)
4.5		19465.123(0)	19452.521(28)
5.5		19462.897(10)	
		15-8 Band	
0.5	17613.528(-12)		
1.5	17617.039(-11)	17610.035(-2)	
2.5	17619.869(1)	17610.035(-12)	17603.032(-2)
3.5	17621.977(-19)	17609.370(5)	17599.558(13)
4.5		17607.991(-3)	17595.379(15)
5.5		17605.944(8)	
6.5		17603.189(-7)	
		16-7 Band	
0.5	20871.590(0)		
1.5	20874.983(3)	20868.052(1)	
2.5	20877.606(-2)	20867.908(2)	20860.983(6)
3.5	20879.472(-5)	20866.998(0)	20857.298(3)
4.5		20865.301(-31)	
5.5		20862.909(0)	
		16-8 Band	
0.5	19014.099(-4)		
1.5	19017.510(-19)	19010.591(-9)	
2.5		19010.531(5)	19003.597(1)
3.5		19009.728(3)	19000.035(12)
4.5		19008.182(-20)	18995.713(-11)
5.5			18990.725(23)
		16-9 Band	
0.5	17183.204(-27)		
1.5	17186.665(-28)	17179.743(-20)	
2.5		-	17172.823(-10)
3.5		17179.038(-31)	17169.353(-14)
		19-10 Band	
0.5	19420.711(1)		
1.5	19423.915(-21)	19417.284(4)	
2.5	19426.392(-7)	19417.075(-3)	19410.435(14)
3.5	19428.095(-4)	19416.109(-3)	19406.813(21)
4.5		19414.382(-4)	19402.399(0)
5.5		19411.912(10)	
		19-11 Band	
0.5	17643.366(-18)		
1.5	17646.651(8)	17639.996(10)	
2.5	17649.162(-13)	17639.860(6)	17633.209(10)
3.5		17639.017(20)	17629.704(28)
4.5			17625.418(-11)

TABLE I—*Continued*

J	R_{11}(J)	Q_{11}(J)	P_{11}(J)
		20-10 Band	
1.5	20716.976(-5)	20710.404(-14)	
2.5	20719.323(9)	20710.135(12)	20703.563(4)
3.5		20709.025(-2)	20699.778(-59)
		20-11 Band	
0.5	18936.501(-22)		
1.5	18939.665(-23)	18933.126(1)	
2.5		18932.895(-5)	
3.5		18931.912(0)	18922.744(22)
		21-10 Band	
0.5	21979.393(-2)		
1.5	21982.470(10)	21975.969(5)	
2.5		21975.576(-26)	21969.112(6)
3.5		21974.422(9)	21965.301(-15)
4.5			21960.722(21)
5.5			21955.256(-3)
		21-11 Band	
0.5	20202.059(-10)		
1.5	20205.165(-2)	20198.672(1)	
2.5	20207.463(-13)	20198.363(-16)	20191.902(20)
3.5			20188.196(-6)
4.5			20183.693(-38)

were populated. In the strongest bands transitions with J up to 6.5 were observed. Because the spin–rotation constants, γ_v, for the vibrational levels of the $X^2\Sigma^+$ state are very small (of the order of 10^{-3} cm^{-1}) the spin-splitting is not resolved. Hence in the present spectrum, instead of the expected six branches of the $^2\Pi_{3/2}$–$^2\Sigma$ subband, only the branches R_{11}, Q_{11}, and P_{11} were observed. In most of the bands the Q_{11} head was clearly observed, but because the higher rotational levels were not excited the R_{11} heads were not seen. As an illustration the rotational structure of the 8–3 band of the red system is shown in Fig. 1.

The computer program PC-DECOMP, developed by J. W. Brault at the National Solar Observatory, was used to measure the line positions. The rotational line profiles were fitted to Voigt line shape functions. The strong lines show "ringing" caused by the $(\sin x/x)$ lineshape function of the Fourier transform spectrometer. The ringing was eliminated by using the "filter fitting" option. The signal-to-noise ratio for strongest lines was about 20. The rotational quantum numbers and the vacuum wavenumbers of the spectral lines of all the 27 bands analyzed in the present work are listed in Table I.

Initially, the band-by-band fits of the wavenumber data of Table I were made using the effective Hamiltonian of Brown *et al.* (*43*). The Hamiltonian matrix elements for a $^2\Pi$ state are explicitly listed by Amiot *et al.* (*44*), while the $^2\Sigma^+$ matrix elements are provided by Douay *et al.* (*45*).

In our earlier work on CN (*1*), 17 bands of the violet system ($B^2\Sigma^+$–$X^2\Sigma^+$) with $v' = 0$ to 9 and $v'' = 0$ to 8 (0–0 through 7–7 and 1–0 through 9–8) were analyzed. These data were combined with all of the available microwave data for $v = 0$ to 10

TABLE II

Molecular Constants (in cm^{-1}) for the $X^2\Sigma^+$ State of the CN Molecule

Vibrational Level	T_v	B_v	D_v /10^{-6}	H_v /10^{-12}	γ_v /10^{-3}
0	0.0	1.89109067(19)	6.4094(47)	4.9(14)	7.25517(63)
1	2042.41851(68)	1.87366616(21)	6.4157(45)	4.1(13)	7.17398(89)
2	4058.54467(77)	1.85618743(21)	6.4239(44)	3.3(13)	7.0833(14)
3	6048.33680(93)	1.83865304(26)	6.4355(43)	3.4(12)	6.9819(16)
4	8011.7554(11)	1.82105956(34)	6.4403(26)	-	6.8645(16)
5	9948.7499(23)	1.80340517(99)	6.58(13)	-	6.7208(17)
6	11859.2870(31)	1.78568568(62)	6.545(75)	-	6.5436(16)
7	13743.3235(30)	1.76789664(76)	6.207(98)	-	6.3137(16)
8	15600.8106(32)	1.75004005(47)	6.479(31)	-	6.0126(14)
9	17431.6828(36)	1.7321008(14)	6.494(82)	-	5.6139(30)
10	19235.8808(69)	1.714045(59)	6.4(33)	-	5.2322(30)
11	21013.2066(73)	1.69528(39)	7.5(40)	-	14.9(35)

TABLE III

Molecular Constants (in cm^{-1}) for the $A^2\Pi_i$ State of the CN Molecule

Vibrational Level	T_v[a]	A_v[b]	B_v
8	22700.6453(36)	-51.859	1.567449(27)
9	24283.3107(37)	-51.731	1.549926(69)
10	25840.2065(37)	-51.595	1.53162(21)
11	27371.2601(44)	-51.453	1.51409(18)
12	28876.4136(39)	-51.304	1.49600(19)
13	30355.5738(38)	-51.148	1.47876(17)
14	31808.6885(45)	-50.986	1.45847(27)
15	33235.5516(32)	-50.816	1.441006(58)
16	34636.0772(32)	-50.641	1.423341(42)
19	38677.6346(79)	-50.073	1.36635(24)
20	39970.7276(74)	-49.870	1.34690(13)
21	41236.2086(82)	-49.661	1.33306(28)

[a] The term values listed here are relative to the v=0 level of the $X^2\Sigma^+$ state.

[b] Calculated from the expression $A_v = -52.6846+0.0686(v+1/2)+0.00335(v+1/2)^2$ given by Kotlar et al.(32) and held fixed in our fit.

TABLE IV

Molecular Constants (in cm^{-1}) for the $B^2\Sigma^+$ State of the CN Molecule

Vibrational Level	T_v[a]	B_v	D_v /10^{-6}	γ_v /10^{-3}
0	25797.8693(10)	1.958728(12)	6.606(23)	17.155(91)
1	27921.4652(12)	1.937995(19)	6.654(51)	18.03(13)
2	30004.8966(15)	1.916649(49)	7.68(32)	18.29(19)
3	32045.9383(17)	1.894004(62)	5.42(54)	24.06(20)
4	34041.9520(20)	1.870330(99)	6.38(89)	18.92(39)
5	35990.0220(52)	1.85158(80)	94.1(219)	11.1(22)
6	37887.3796(31)	1.819169(59)	6.06(49)	24.20(23)
7	39730.4754(31)	1.790946(29)	12.17(17)	6.57(17)
8	41516.5744(35)	1.762140(34)	8.62(18)	31.92(17)
9	43242.9051(35)	1.730417(18)	10.086(54)	6.26(12)
11	46511.3138(78)	1.66477(39)	8.1(38)	24.4(33)

[a] The term values listed here are relative to the v=0 level of the $X^2\Sigma^+$ state.

TABLE V

Comparison of T_v and B_v Values of the $A^2\Pi_i$ State of the CN Molecule (in cm^{-1})

Vibrational Level	T_v			B_v		
	Kotlar et al.[a]	Cerny et al.[a]	This work	Kotlar et al.[a]	Cerny et al.[a]	This work
0	9115.687	9115.686	-	1.70707	1.70712	-
1	10903.414	10903.414	-	1.68979	1.68984	-
2	12665.571	12665.572	-	1.67246	1.67252	-
3	14402.143	14402.148	-	1.65508	1.65515	-
4	16113.117	16113.134	-	1.63765	1.63770	
8	22700.670	-	22700.645	1.56737	-	1.56745
9	24283.333	-	24283.311	1.54966	-	1.54993
10	25840.223	-	25840.207	1.53189	-	1.53162
11	27371.278		27371.260	1.51408	-	1.51409
12	28876.425	-	28876.414	1.49617	-	1.49600

[a] The constants from Kotlar et al. (32) and Cerny et al. (31) are converted from the $\mathbf{R}^2$ Hamiltonian to the $\mathbf{N}^2$ Hamiltonian. See text for details.

TABLE VI

Equilibrium Molecular Constants for the $X^2\Sigma^+$, $A^2\Pi_i$, and $B^2\Sigma^+$ States of CN

Molecular Constant	$X^2\Sigma^+$	$A^2\Pi_i$	$B^2\Sigma^+$
$Y_{10}(\omega_e)$	2068.648(11)	1813.235(29)	2160.38(31)
$-Y_{20}(\omega_e x_e)$	13.0971(68)	12.7511(80)	17.744(78)
$Y_{30}(\omega_e y_e)$	-0.0124(17)	-0.00666(90)	-0.4670(54)
$Y_{40}(\omega_e z_e)$	$0.70(18)\times10^{-3}$	$-30.400(45)\times10^{-3}$	-
Y_{50}	$-0.323(68)\times10^{-4}$	$-0.1865(81)\times10^{-4}$	-
$Y_{01}(B_e)$	1.89978316(67)	1.71562(11)	1.96879(13)
$-Y_{11}(\alpha_e)$	0.0173720(12)	0.017120(31)	0.01996(18)
$Y_{21}(\gamma_e)$	$-0.2586(56)\times10^{-4}$	$-0.366(18)\times10^{-4}$	$-0.331(44)\times10^{-3}$
Y_{31}	$-0.211(99)\times10^{-6}$	-	$-0.220(29)\times10^{-4}$
Y_{41}	$-0.161(57)\times10^{-7}$	-	-
r_e(Å)	1.17180749(21)	1.233098(40)	1.151088(38)

Note: Constants are in inverse centimeters unless stated otherwise.

of the $X^2\Sigma^+$ (*39, 46–48*) in a final fit. Rehfuss *et al.* (*2*), in their investigation of the violet system, analyzed the 0–0 through 13–13 bands, except the 5–5, 10–10, and 12–12 bands, and the 0–1 through 9–10 bands, except the 5–6 band. For the final fit of the present work, in addition to all the data used in our earlier work and the present data from the 27 bands of red system, we also used the vibration–rotation data of Davis *et al.* (*38*) (1–0, 2–1, 3–2, 4–3, 2–0, 3–1, and 4–2 bands of the $X^2\Sigma^+$ state)

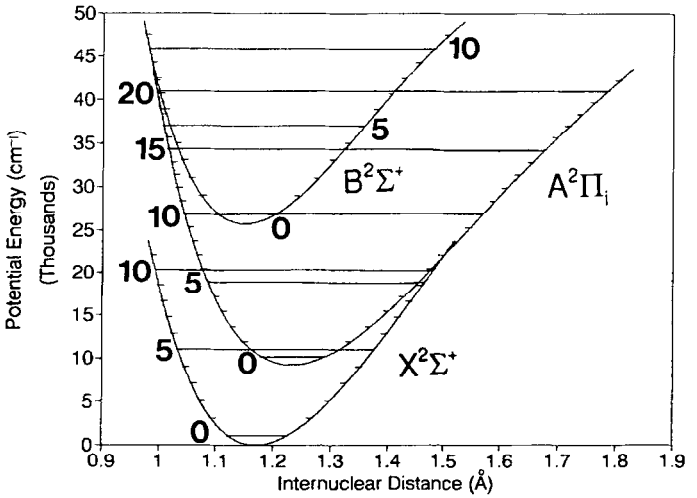

FIG. 2. The RKR potential energy curves of the $B^2\Sigma^+$, $A^2\Pi$, and $X^2\Sigma^+$ states of CN.

TABLE VII

RKR Turning Points for the $X^2\Sigma^+$, $A^2\Pi_i$, and $B^2\Sigma^+$ States of the CN Molecule

Vibrational Level	$X^2\Sigma^+$			$A^2\Pi_i$			$B^2\Sigma^+$		
	$E_v(cm^{-1})$	$R_{min}(Å)$	$R_{max}(Å)$	$E_v(cm^{-1})$	$R_{min}(Å)$	$R_{max}(Å)$	$E_v(cm^{-1})$	$R_{min}(Å)$	$R_{max}(Å)$
0	1031.048	1.12432	1.22503	10146.737	1.18253	1.29013	26828.963	1.10480	1.20341
1	3073.465	1.09279	1.26816	11934.450	1.14912	1.33660	28952.338	1.07425	1.24634
2	5089.594	1.07254	1.30016	13696.611	1.12774	1.37123	31036.021	1.05473	1.27871
3	7079.386	1.05689	1.32771	15433.194	1.11128	1.40115	33077.210	1.03975	1.30707
4	9042.800	1.04394	1.35273	17144.178	1.09768	1.42840	35073.102	1.02742	1.33339
5	10979.797	1.03280	1.37610	18829.544	1.08602	1.45394	37020.896	1.01689	1.35859
6	12890.337	1.02298	1.39832	20489.270	1.07576	1.47829	38917.788	1.00770	1.38322
7	14774.377	1.01418	1.41970	22123.335	1.06659	1.50178	40760.977	0.99956	1.40766
8	16631.864	1.00619	1.44045	23731.709	1.05829	1.52463	42547.661	0.99227	1.43221
9	18462.733	0.99888	1.46071	25314.359	1.05071	1.54700	44275.037	0.98570	1.45711
10	20266.903	0.99213	1.48061	26871.240	1.04373	1.56902	45940.303	0.97976	1.48259
11	22044.273	0.98587	1.50023	28402.295	1.03726	1.59078	47540.657	0.97436	1.50888
12				29907.455	1.03123	1.61237			
13				31386.633	1.02560	1.63384			
14				32839.725	1.02030	1.65525			
15				34266.606	1.01532	1.67665			
16				35667.128	1.01060	1.69810			
17				37041.117	1.00613	1.71962			
18				38388.374	1.00187	1.74126			
19				39708.668	0.99781	1.76307			
20				41001.738	0.99393	1.78508			
21				42267.287	0.99020	1.80732			

and the data from Rehfuss *et al.* (*2*) on the 0–1 through 9–10 bands, as well as the 8–8, 9–9, and 11–11 bands of the violet system. All this experimental data, about 2000 transitions, were fitted together simultaneously in a nonlinear least-squares fit and a set of 119 parameters were estimated. The variance of this global fit was 1.121. These 119 parameters include T_v, B_v, D_v, H_v (v = 0, 1, 2, and 3 only), and γ_v for the v = 0 to 11 of the $X^2\Sigma^+$ state (51 parameters); T_v and B_v for v = 8 to 16, 19 to 21 of the $A^2\Pi_i$ state (24 parameters); and T_v, B_v, D_v, and γ_v for v = 0 to 9, 11 of the $B^2\Sigma^+$ state (44 parameters). All these parameters, along with one standard deviation

TABLE VIII

Franck–Condon Factors for the Bands of the Red ($A^2\Pi_i$–$X^2\Sigma^+$) System of CN

v'\v"	0	1	2	3	4	5	6	7	8	9	10	11
0	4.95E-01	3.72E-01	1.13E-01	1.79E-02	1.60E-03	8.18E-05	2.30E-06	3.18E-08	1.68E-10	8.78E-14	9.80E-16	2.24E-16
1	3.21E-01	4.35E-02	3.48E-01	2.24E-01	5.54E-02	6.79E-03	4.41E-04	1.50E-05	2.43E-07	1.44E-09	5.50E-13	4.10E-14
2	1.27E-01	2.39E-01	1.31E-02	2.07E-01	2.88E-01	1.06E-01	1.72E-02	1.38E-03	5.60E-05	1.04E-06	6.72E-09	7.11E-13
3	4.05E-02	1.95E-01	9.71E-02	9.18E-02	8.11E-02	2.96E-01	1.61E-01	3.37E-02	3.30E-03	1.56E-04	3.29E-06	2.20E-08
4	1.14E-02	9.56E-02	1.82E-01	1.45E-02	1.51E-01	1.29E-02	2.59E-01	2.11E-01	5.63E-02	6.63E-03	3.63E-04	8.46E-06
5	3.01E-03	3.66E-02	1.35E-01	1.22E-01	2.41E-03	1.58E-01	1.60E-03	1.98E-01	2.48E-01	8.41E-02	1.18E-02	7.36E-04
6	7.66E-04	1.23E-02	6.84E-02	1.42E-01	5.71E-02	3.27E-02	1.25E-01	2.76E-02	1.29E-01	2.68E-01	1.16E-01	1.91E-02
7	1.92E-04	3.79E-03	2.85E-02	9.59E-02	1.21E-01	1.37E-02	7.26E-02	7.62E-02	6.78E-02	6.95E-02	2.71E-01	1.49E-01
8	4.79E-05	1.12E-03	1.05E-02	4.91E-02	1.10E-01	8.34E-02	1.01E-06	9.97E-02	3.23E-02	1.04E-01	2.66E-02	2.58E-01
9	1.21E-05	3.22E-04	3.61E-03	2.15E-02	6.94E-02	1.07E-01	4.38E-02	1.09E-02	1.05E-01	6.02E-03	1.25E-01	4.28E-03
10	3.07E-06	9.16E-05	1.18E-03	8.49E-03	3.57E-02	8.41E-02	8.98E-02	1.44E-02	3.45E-02	9.08E-02	4.53E-04	1.27E-01
11	7.98E-07	2.61E-05	3.79E-04	3.15E-03	1.62E-02	5.09E-02	8.95E-02	6.36E-02	8.53E-04	5.87E-02	6.47E-02	1.20E-02
12	2.12E-07	7.50E-06	1.20E-04	1.13E-03	6.76E-03	2.64E-02	6.41E-02	8.43E-02	3.61E-02	3.07E-03	7.43E-02	3.64E-02
13	5.77E-08	2.18E-06	3.78E-05	3.93E-04	2.68E-03	1.24E-02	3.80E-02	7.24E-02	7.00E-02	1.42E-02	1.64E-02	7.75E-02
14	1.61E-08	6.44E-07	1.20E-05	1.35E-04	1.03E-03	5.42E-03	1.99E-02	4.92E-02	7.38E-02	5.04E-02	2.09E-03	3.40E-02
15	4.58E-09	1.93E-07	3.82E-06	4.64E-05	3.85E-04	2.27E-03	9.63E-03	2.89E-02	5.79E-02	6.79E-02	3.00E-02	6.34E-04
16	1.33E-09	5.90E-08	1.23E-06	1.60E-05	1.43E-04	9.24E-04	4.41E-03	1.54E-02	3.81E-02	6.23E-02	5.59E-02	1.31E-02
17	3.88E-10	1.82E-08	4.01E-07	5.50E-06	5.27E-05	3.69E-04	1.94E-03	7.66E-03	2.24E-02	4.63E-02	6.16E-02	4.04E-02
18	1.13E-10	5.64E-09	1.31E-07	1.91E-06	1.94E-05	1.46E-04	8.33E-04	3.64E-03	1.21E-02	3.00E-02	5.18E-02	5.53E-02
19	3.16E-11	1.73E-09	4.31E-08	6.63E-07	7.14E-06	5.72E-05	3.51E-04	1.68E-03	6.23E-03	1.77E-02	3.72E-02	5.36E-02
20	8.18E-12	5.15E-10	1.40E-08	2.30E-07	2.63E-06	2.23E-05	1.47E-04	7.56E-04	3.07E-03	9.79E-03	2.39E-02	4.28E-02
21	1.80E-12	1.44E-10	4.42E-09	7.90E-08	9.64E-07	8.70E-06	6.07E-05	3.35E-04	1.47E-03	5.17E-03	1.43E-02	3.01E-02

TABLE IX

Franck–Condon Factors for the Bands of the LeBlanc ($B^2\Sigma^+$–$A^2\Pi_i$) System of the CN Molecule

v'\v''	0	1	2	3	4	5	6	7	8	9	10
0	2.82E-01	3.19E-01	2.13E-01	1.09E-01	4.79E-02	1.90E-02	7.05E-03	2.50E-03	8.60E-04	2.90E-04	9.68E-05
1	3.98E-01	1.86E-02	6.32E-02	1.62E-01	1.56E-01	1.03E-01	5.48E-02	2.56E-02	1.10E-02	4.45E-03	1.73E-03
2	2.34E-01	1.47E-01	1.43E-01	2.47E-03	4.92E-02	1.17E-01	1.21E-01	8.69E-02	5.10E-02	2.63E-02	1.24E-02
3	7.26E-02	3.02E-01	9.20E-03	1.48E-01	5.71E-02	8.13E-04	5.11E-02	9.69E-02	9.74E-02	7.23E-02	4.47E-02
4	1.23E-02	1.69E-01	2.39E-01	1.55E-02	7.80E-02	9.98E-02	1.58E-02	8.21E-03	5.45E-02	8.39E-02	8.05E-02
5	1.01E-03	4.02E-02	2.44E-01	1.41E-01	6.77E-02	1.95E-02	9.59E-02	4.98E-02	1.11E-03	1.86E-02	5.63E-02
6	2.47E-05	3.96E-03	7.93E-02	2.84E-01	6.29E-02	1.04E-01	6.39E-05	6.43E-02	7.09E-02	1.67E-02	1.50E-03
7	9.99E-08	8.33E-05	8.87E-03	1.23E-01	2.96E-01	1.93E-02	1.11E-01	9.34E-03	3.07E-02	7.11E-02	3.70E-02
8	9.15E-08	2.29E-06	1.31E-04	1.48E-02	1.65E-01	2.91E-01	2.55E-03	9.75E-02	2.87E-02	8.87E-03	5.70E-02
9	7.60E-11	6.19E-07	1.68E-05	9.84E-05	2.00E-02	2.02E-01	2.84E-01	1.15E-04	7.52E-02	4.57E-02	5.00E-04
10	4.13E-10	2.99E-09	1.87E-06	6.96E-05	6.84E-06	2.27E-02	2.34E-01	2.82E-01	2.02E-03	5.33E-02	5.56E-02
11	1.25E-14	4.02E-09	8.88E-08	2.81E-06	1.95E-04	1.41E-04	2.13E-02	2.57E-01	2.93E-01	2.94E-03	3.56E-02

v'\v''	11	12	13	14	15	16	17	18	19	20	21
0	3.22E-05	1.07E-05	3.58E-06	1.21E-06	4.12E-07	1.42E-07	4.94E-08	1.74E-08	6.14E-09	2.16E-09	7.54E-10
1	6.53E-04	2.43E-04	8.94E-05	3.28E-05	1.20E-05	4.43E-06	1.64E-06	6.10E-07	2.28E-07	8.55E-08	3.20E-08
2	5.51E-03	2.35E-03	9.69E-04	3.93E-04	1.57E-04	6.25E-05	2.48E-05	9.83E-06	3.90E-06	1.55E-06	6.15E-07
3	2.45E-02	1.24E-02	5.92E-03	2.71E-03	1.20E-03	5.24E-04	2.25E-04	9.58E-05	4.06E-05	1.71E-05	7.22E-06
4	6.01E-02	3.84E-02	2.20E-02	1.17E-02	5.92E-03	2.88E-03	1.36E-03	6.28E-04	2.86E-04	1.29E-04	5.80E-05
5	7.35E-02	6.72E-02	5.01E-02	3.26E-02	1.94E-02	1.08E-02	5.69E-03	2.90E-03	1.44E-03	7.03E-04	3.38E-04
6	2.80E-02	5.58E-02	6.43E-02	5.64E-02	4.17E-02	2.76E-02	1.68E-02	9.68E-03	5.33E-03	2.84E-03	1.47E-03
7	2.15E-03	8.50E-03	3.47E-02	5.33E-02	5.58E-02	4.72E-02	3.48E-02	2.33E-02	1.45E-02	8.60E-03	4.90E-03
8	5.02E-02	1.26E-02	4.53E-04	1.68E-02	3.83E-02	4.93E-02	4.81E-02	3.95E-02	2.90E-02	1.96E-02	1.24E-02
9	3.85E-02	5.33E-02	2.48E-02	1.54E 03	5.33E 03	2.37E-02	3.92E-02	4.45E-02	4.10E 02	3.29E-02	2.40E-02
10	1.22E-03	2.23E-02	4.89E-02	3.36E-02	7.45E-03	4.68E-04	1.21E-02	2.81E-02	3.79E-02	3.92E-02	3.45E-02
11	5.89E-02	5.89E-03	1.11E-02	4.02E-02	3.76E-02	1.43E-02	4.64E-04	4.71E-03	1.81E-02	2.99E-02	3.50E-02

error, are listed in the Tables II, III, and IV for the $X^2\Sigma^+$, $A^2\Pi_i$, and $B^2\Sigma^+$ states, respectively. The constants in these tables supercede those reported in our previous publication on CN (*1*). In Table I, the observed minus calculated values obtained for the line positions of the red system using the constants listed in Tables II and III are also listed. Table III also contains the A_v values, which were calculated from the expression given by Kotlar *et al.* (*32*), and held fixed in our fit. Because only the $A^2\Pi_{3/2}$–$X^2\Sigma^+$ subband was observed in the present work, it was necessary to use the A_v expression of Kotlar *et al.* (*32*).

The present data for the $A^2\Pi_i$ state covers the vibrational levels from $v = 8$ to 21. In order to estimate the equilibrium molecular constants the data for the lower vibrational levels would be very useful. Cerny *et al.* (*31*) analyzed the red system in the spectral range 4000–11 000 cm^{-1} and extracted molecular constants for the first five

TABLE X

Franck–Condon Factors for the Bands of the Violet ($B^2\Sigma^+$–$X^2\Sigma^+$) System of the CN Molecule

v'\v''	0	1	2	3	4	5	6	7	8	9	10	11
0	9.19E-01	7.47E-02	5.45E-03	3.49E-04	2.15E-05	1.26E-06	6.82E-08	3.46E-09	2.07E-10	2.64E-11	7.49E-12	243E-12
1	7.92E-02	7.78E-01	1.27E-01	1.43E-02	1.23E-03	9.66E-05	6.97E-06	4.66E-07	2.91E-08	2.02E-09	2.44E-10	626E-11
2	1.34E-03	1.44E-01	6.66E-01	1.60E-01	2.50E-02	2.70E-03	2.58E-04	2.22E-05	1.77E-06	1.33E-07	1.06E-08	129E-09
3	7.28E-07	3.20E-03	1.96E-01	5.82E-01	1.78E-01	3.59E-02	4.67E-03	5.29E-04	5.30E-05	4.93E-06	4.31E-07	396E-08
4	8.82E-07	1.36E-05	4.78E-03	2.38E-01	5.21E-01	1.82E-01	4.62E-02	6.94E-03	9.15E-04	1.04E-04	1.11E-05	1.12E-06
5	3.27E-09	4.90E-06	8.32E-05	5.42E-03	2.69E-01	4.84E-01	1.76E-01	5.51E-02	9.26E-03	1.40E-03	1.79E-04	216E-05
6	7.76E-10	5.56E-10	1.46E-05	3.09E-04	4.73E-03	2.91E-01	4.68E-01	1.61E-01	6.25E-02	1.13E-02	1.96E-03	274E-04
7	5.00E-11	9.08E-09	5.34E-08	2.92E-05	8.49E-04	2.82E-03	3.01E-01	4.72E-01	1.38E-01	6.87E-02	1.28E-02	254E-03
8	9.39E-12	1.06E-10	4.56E-08	8.08E-07	3.92E-05	1.88E-03	6.24E-04	2.99E-01	4.96E-01	1.11E-01	7.43E-02	133E-02
9	5.79E-15	1.14E-10	3.75E-11	1.24E-07	4.70E-06	2.88E-05	3.48E-03	2.90E-04	2.80E-01	5.39E-01	7.99E-02	805E-02
10	1.37E-13	9.67E-13	5.90E-10	5.15E-09	1.60E-07	1.69E-05	1.86E-06	5.36E-03	5.41E-03	2.41E-01	5.96E-01	483E-02
11	3.46E-14	1.06E-12	3.58E-11	1.43E-09	4.70E-08	1.74E-08	4.16E-05	5.16E-05	6.68E-03	2.05E-02	1.80E-01	657E-01

($v = 0$ to 4) vibrational levels of the $A^2\Pi$ state. However, they used the $\mathbf{R}^2$ Hamiltonian of Zare *et al.* (*49*), while we used the $\mathbf{N}^2$ Hamiltonian of Brown *et al.* (*43*). The B_v and T_v constants of Cerny *et al.* (*31*) and Kotlar *et al.* (*32*) were adjusted using the approximate formulae given by Amiot *et al.* (*44*) and Foster (*50*),

$$B_v(\mathbf{N}^2) = B_v(\mathbf{R}^2) + q_v(\mathbf{R}^2)/2 \quad (1)$$

and

$$T_v(\mathbf{N}^2) = T_v(\mathbf{R}^2) - B_v(\mathbf{N}^2) \quad (2)$$

and listed in Table V. The agreement between the values obtained in the present work and those of Kotlar *et al.* listed in this table is quite satisfactory.

The B_v and T_v values of Tables II, IV, and III along with Cerny's data (Table V) were fitted to the usual polynomial expansions (*51*) in powers of $(v + 1/2)$ to obtain sets of equilibrium constants. From these fits the equilibrium constants B_e, α_e, γ_e, etc., and ω_e, $\omega_e x_e$, $\omega_e y_e$, etc., were estimated for the X, A, and B states and reported in Table VI. These fits were not satisfactory because of the global perturbations present in the X, A, and B states of CN, but they are the best constants possible without a complete deperturbation. The equilibrium internuclear distance, r_e, is calculated using the corresponding B_e value for the three states and is given in the same table.

The RKR potential energy curves for the X, A, and B states were calculated using the equilibrium constants given in Table VI, and the curves obtained are shown in Fig. 2. The RKR turning points for the observed vibrational levels of the three states are listed in Table VII. Since rotational analyses for the high vibrational levels of the $A^2\Pi$ state are not available in the literature, our work allows the RKR curve to be extended up to $v = 21$. These RKR potentials were used to calculate Franck–Condon factors for the bands of the red ($A^2\Pi_i$–$X^2\Sigma^+$), LeBlanc ($B^2\Sigma^+$–$A^2\Pi_i$), and violet ($B^2\Sigma^+$–$X^2\Sigma^+$) systems and are listed in Tables VIII, IX, and X, respectively.

ACKNOWLEDGMENTS

The National Solar Observatory is operated by the Association for Research in Astronomy, Inc., under contract with the National Science Foundation. We thank J. Wagner, C. Plymate, and G. Ladd for assistance in recording the spectra. We also thank R. W. Nicholls for providing Refs. (*28*) and (*29*). This work was supported by the NASA Origins of the Solar System Research Program and the Natural Sciences and Engineering Research Council of Canada (NSERC). Some support was provided by the Phillips Laboratory/Propulsion Directorate, Edwards Air Force Base, CA.

RECEIVED: May 11, 1992

REFERENCES

1. C. V. V. PRASAD, P. F. BERNATH, C. FRUM, AND R. ENGLEMAN, JR., *J. Mol. Spectrosc.* **151**, 459–473 (1992).
2. B. D. REHFUSS, M. H. SUH, T. A. MILLER, AND V. E. BONDYBEY, *J. Mol. Spectrosc.* **151**, 437–458 (1992).
3. E. C. RICHARD, D. J. DONALDSON, AND V. VAIDA, *Chem. Phys. Lett.* **157**, 295–299 (1989).
4. D. L. LAMBERT, *Mon. Not. R. Astron. Soc.* **138**, 143–179 (1968); C. SNEDEN AND D. L. LAMBERT, *Astrophys. J.* **259**, 381–391 (1982).
5. D. L. LAMBERT, J. A. BROWN, K. H. HINKLE, AND H. R. JOHNSON, *Astrophys. J.* **284**, 223–237 (1984).
6. A. WOOTTEN, S. M. LICHTEN, R. SAHAI, AND P. G. WANNIER, *Astrophys. J.* **257**, 151–160 (1982).
7. J. R. JOHNSON, U. FINK, AND H. P. LARSON, *Astrophys. J.* **270**, 769–777 (1983).
8. B. E. TURNER AND R. H. GAMMON, *Astrophys. J.* **198**, 71–89 (1975).
9. M. GERIN, F. COMBES, P. ENCRENAZ, R. LINKE, J. L. DESTOMBES, AND C. DEMUYNCK, *Astron. Astrophys.* **136**, L17–L20 (1984).

10. D. M. MEYER AND M. JURA, *Astrophys. J.* **276,** L1–L3 (1984); **297,** 119–132 (1985).
11. D. C. MORTON, *Astrophys. J.* **197,** 85–115 (1975).
12. D. L. LAMBERT, Y. SHEFFER, AND P. CRANE, *Astrophys. J.* **359,** L19–L22 (1990); S. R. FEDERMAN, A. C. DANKS, AND D. L. LAMBERT, *Astrophys. J.* **287,** 219–227 (1984).
13. P. CRANE, D. J. HEGYI, N. MANDOLESI, AND A. C. DANKS, *Astrophys. J.* **309,** 822–827 (1986).
14. J. H. BLACK AND E. F. VAN DISHOECK, *Astrophys. J.* **331,** 986–998 (1988).
15. D. M. MEYER, K. C. ROTH, AND I. HAWKINS, *Astrophys. J.* **343,** L1–L4 (1989).
16. P. G. CARRICK, C. R. BRAZIER, P. F. BERNATH, AND P. C. ENGELKING, *J. Am. Chem. Soc.* **109,** 5100–5102 (1987).
17. C. R. BRAZIER, P. G. CARRICK, AND P. F. BERNATH, *J. Chem. Phys.* **96,** 919–926 (1992).
18. N. OLIPHANT, A. LEE, P. F. BERNATH, AND C. R. BRAZIER, *J. Chem. Phys.* **92,** 2244–2247 (1990).
19. P. C. ENGELKING, *Rev. Sci. Instrum.* **57,** 2274–2277 (1986).
20. T. HEURLINGER, *Z. Phys.* **1,** 82–91 (1920).
21. R. S. MULLIKEN, *Nature* **114,** 858–859 (1924).
22. R. K. ASUNDI AND J. W. RYDE, *Nature* **124,** P57 (1929).
23. G. HERZBERG AND J. G. PHILLIPS, *Astrophys. J.* **108,** 163–166 (1948).
24. A. E. DOUGLAS AND P. M. ROUTLEY, *Astrophys. J. Suppl.* **1,** 295–318 (1955).
25. F. J. LEBLANC, *J. Chem. Phys.* **48,** 1980–1984 (1968).
26. F. A. JENKINS, Y. K. ROOTS, AND R. S. MULLIKEN, *Phys. Rev.* **39,** 16–41 (1932).
27. S. P. DAVIS AND J. G. PHILLIPS, "The Red System ($A^2\Pi$–$X^2\Sigma$) of the CN Molecule," Berkeley Analyses of Molecular Spectra, Univ. of California Press, Berkeley, 1963.
28. B. BROCKLEHURST, G. R. HEBERT, S. H. INNANEN, R. M. SEEL, AND R. W. NICHOLLS, "Identification Atlas of Molecular Spectra, Vol. 8, The CN $A^2\Pi_i$–$X^2\Sigma^+$ Red System," Centre for Research in Experimental Space Science, York University, Toronto, Ontario, Canada, 1971.
29. B. BROCKLEHURST, G. R. HEBERT, S. H. INNANEN, R. M. SEEL AND R. W. NICHOLLS, "Identification Atlas of Molecular Spectra, Vol. 9, The CN $B^2\Sigma^+$–$X^2\Sigma^+$ Violet System," Centre for Research in Experimental Space Science, York University, Toronto, Ontario, Canada, 1972.
30. K. P. HUBER AND G. HERZBERG, "Constants of Diatomic Molecules," Van Nostrand-Reinhold, New York, 1979.
31. D. CERNY, R. BACIS, G. GUELACHVILI, AND F. ROUX, *J. Mol. Spectrosc.* **73,** 154–167 (1978).
32. A. J. KOTLAR, R. W. FIELD, J. Z. STEINFELD, AND J. A. COXON, *J. Mol. Spectrosc.* **80,** 86–108 (1980).
33. Y. OZAKI, T. NAGATA, K. SUZUKI, T. KONDOW, AND K. KUCHITSU, *Chem. Phys.* **80,** 73–84 (1983); Y. OZAKI, H. ITO, K. SUZUKI, T. KONDOW, AND K. KUCHITSU, *Chem. Phys.* **80,** 85–94 (1983).
34. H. ITO, Y. OZAKI, T. NAGATA, T. KONDOW, AND K. KUCHITSU, *Can. J. Phys.* **62,** 1586–1596 (1984).
35. H. ITO, Y. OZAKI, K. SUZUKI, T. KONDOW, AND K. KUCHITSU, *Chem. Phys. Lett.* **139,** 581–584 (1987).
36. H. ITO, Y. FUKUDA, Y. OZAKI, T. KONDOW, AND K. KUCHITSU, *J. Mol. Spectrosc.* **121,** 84–90 (1987).
37. H. ITO, Y. OZAKI, K. SUZUKI, T. KONDOW, AND K. KUCHITSU, *J. Mol. Spectrosc.* **127,** 143–155; 283–303 (1988).
38. S. P. DAVIS, M. C. ABRAMS, M. L. P. RAO, AND J. W. BRAULT, *J. Opt. Soc. Am. B* **8,** 198–200 (1991); and unpublished data.
39. H. ITO, K. KUCHITSU, S. YAMAMOTO, AND S. SAITO, *Chem. Phys. Lett.* **186,** 539–546 (1991).
40. M. KAKIMOTO AND T. KASUYA, *J. Mol. Spectrosc.* **94,** 380–392 (1982).
41. T. SUZUKI, S. SAITO, AND E. HIROTA, *J. Mol. Spectrosc.* **113,** 399–409 (1985).
42. M. C. CURTIS AND P. J. SARRE, *J. Mol. Spectrosc.* **114,** 427–435 (1985).
43. J. M. BROWN, E. A. COLBOURN, J. K. G. WATSON, AND F. D. WAYNE, *J. Mol. Spectrosc.* **74,** 425–436 (1979).
44. C. AMIOT, J.-P. MAILLARD, AND J. CHAUVILLE, *J. Mol. Spectrosc.* **87,** 196–218 (1981).
45. M. DOUAY, S. A. ROGERS, AND P. F. BERNATH, *Mol. Phys.* **64,** 425–436 (1988).
46. T. A. DIXON AND R. C. WOODS, *J. Chem. Phys.* **67,** 3956–3964 (1977).
47. D. A. SKATRUD, F. C. DELUCIA, G. A. BLAKE, AND K. V. L. N. SASTRY, *J. Mol. Spectrosc.* **99,** 35–46 (1983).
48. M. A. JOHNSON, M. L. ALEXANDER, I. HERTEL, AND W. C. LINEBERGER, *Chem. Phys. Lett.* **105,** 374–379 (1984).
49. R. N. ZARE, A. L. SCHMELTEKOPF, W. J. HARROP, AND D. L. ALBRITTON, *J. Mol. Spectrosc.* **46,** 37–66 (1973).
50. S. C. FOSTER, *J. Mol. Spectrosc.* **137,** 430–431 (1989).
51. G. HERZBERG, "Spectra of Diatomic Molecules," Van Nostrand-Reinhold, New York, 1950.